Lasers in Medical Science (2019) 34:1019–1029
https://doi.org/10.1007/s10103-018-2692-5

ORIGINAL ARTICLE

Essential Role of mTOR Signaling in Human Retinal Pigment Epithelial Cell Regeneration After Laser Photocoagulation

Sanjar Batirovich Madrakhimov[1,2] · Jin Young Yang[1,2] · Ha Yan Park[2] · Tae Kwann Park[1,2,3,4]

Received: 20 August 2018 / Accepted: 19 November 2018 / Published online: 29 November 2018

Abstract

This study assessed the role of mechanistic target of rapamycin (mTOR) pathway in the human adult retinal pigment epithelial (ARPE) cell response after laser photocoagulation (LP). The effect of mTOR inhibition on ARPE-19 cell was investigated by rapamycin treatment after LP. Cell viability and proliferation were explored using MTT and EdU assays, respectively. The expression of mTOR-related proteins and epithelial-mesenchymal transition (EMT) markers was verified by Western blot. Rapamycin retarded the LP area recovery in a dose-dependent manner by the 120 h, while LP+DMSO vehicle-treated cells completely restored the lesion zone ($P \leq 0.01$). ARPE-19 cell viability is significantly lower in LP + rapamycin 80 and 160 ng/ml treated cultures compared to LP control at 120 h ($P \leq 0.001$). LP control group demonstrated significantly more proliferative cells compared to untreated cells at the 72 and 120 h, whereas EdU-positive cell numbers in cultures treated with rapamycin at concentrations of 80 and 160 ng/ml were similar to baseline values ($P \leq 0.01$). mTOR pathway activation is essential for regulation of the RPE cell migration and proliferation after LP. mTOR inhibition with rapamycin effectively blocks the migration and proliferation of the RPE cells. Our results demonstrate that mTOR has an important role in ARPE-19 cell as a regulator of cell behavior under stress conditions, suggesting that mTOR could be a promising therapeutic target for numerous retinal diseases.

Keywords Retinal pigment epithelium (ARPE-19) · mTORC1 · mTORC2 · Sirolimus (rapamycin) · Laser photocoagulation

Introduction

Laser photocoagulation is an effective treatment method for various retinal disorders including diabetic retinopathy, retinal vein occlusion, vascular tumors, and retinopathy of prematurity, and the clinical efficacy of LP was proven by randomized studies (DRS, ETDRS, ETROP) [1–3]. Most laser applications target the RPE cells; laser energy absorbed by melanosomes in the RPE increases the local temperature resulting in protein denaturation and necrosis at the lesion area [4]. However, neighboring cells get thermal and chemo stimulus to induce cellular response upon LP. The RPE cell response to LP is a complex process including migration and proliferation [5], but the underlying mechanisms are poorly understood.

The retinal pigment epithelium (RPE) is a monolayer of epithelial cells located between neural retina and choroid. The RPE cells are involved in various physiological processes, such as maintenance of metabolic homeostasis as a part of the blood-retinal barrier, participation in visual cycle, secretion of neurotrophic, inflammatory and angioregulatory proteins. The failure of the RPE cell functions contributes to various retinal disorders, including age-related macular degeneration (AMD), diabetic retinopathy (DR), and proliferative vitreoretinopathy [6–9]. The underlying mechanisms for pathogenesis of these diseases are complex, including hypoxia and deregulation of growth factors as a cause or effect. While the crucial role of such growth factors

✉ Tae Kwann Park
tkpark@schmc.ac.kr

[1] Department of Interdisciplinary Program in Biomedical Science, Soonchunhyang Graduate School, Bucheon Hospital, Bucheon, South Korea

[2] Laboratory for Translational Research on Retinal and Macular Degeneration, Soonchunhyang University Hospital Bucheon, Bucheon, South Korea

[3] Department of Ophthalmology, Soonchunhyang University Hospital Bucheon, #170, Jomaru-ro, Wonmi-gu, Bucheon 14584, South Korea

[4] Department of Ophthalmology, College of Medicine, Soonchunhyang University, Cheonan, Choongchungnam-do, South Korea

as vascular endothelial growth factor (VEGF), platelet-derived growth factor (PDGF), and pigment epithelium-derived growth factor (PEDF) are widely studied in retinal pathological conditions [10–12], the contribution of mechanistic target of rapamycin (mTOR) pathway remains unclear.

mTOR is an atypical protein kinase from phosphoinositide 3-kinase family, which mediates basic cellular functions such as growth and proliferation. Dysregulation of mTOR signaling is found in various pathological conditions—cancer, obesity, autoimmune disorders, and senescence [13–16]. mTOR signaling functions through two distinct complexes—mTOR complex 1 (mTORC1) and 2 (mTORC2). While the role of rapamycin-sensitive mTORC1 has been disclosed in protein synthesis, autophagy, cell growth, and proliferation, the regulation of actin cytoskeleton and cell survival are the processes known for mTORC2 to be involved [17]. Rapamycin (sirolimus) is a macrolide, which in combination with FK506-binding protein (FKBP12) binds and inhibits mTORC1 in the case of acute treatment [17, 18]. As an inhibitor of mTORC1, rapamycin has a broad therapeutic potential in inhibiting inflammation, angiogenesis, proliferation, and fibrosis, which are involved in the pathogenesis of various ocular disorders.

Several studies have been conducted to assess the role of the mTOR pathway in various eye diseases with neovascular components, such as AMD, DR, retinopathy of prematurity, and corneal neovascularization [19–22]. Previously, it has been reported that activation of the mTOR pathway is required for ARPE-19 cell survival against oxidative damage [23]. However, hydrogen peroxide-induced cell survival signaling pathway may differ from that of in laser-triggered cell response. ARPE-19 is a widely used cell line as an alternative to native RPE due to its epithelial cell morphology and ability to perform many functions of human RPE [24–26]. Recently, we clearly demonstrated that mTOR inhibition by recombinant adeno-associated virus-delivered mTOR-inhibiting short hairpin RNA (rAAV-mTOR shRNA) induces autophagy, reduces inflammation, and suppresses laser-induced choroidal neovascularization in a mouse model for AMD [27]. Although the above studies have repeatedly reported the therapeutic effect of inhibition of the mTOR pathway, the exact function of mTOR signaling in the RPE cell behavior, in the context of retinal pathological conditions, is still unclear. Therefore, this study aimed to assess the role of the mTOR pathway in ARPE-19 cell response to laser photocoagulation by mTORC1 inhibition with rapamycin treatment. Here, we showed that mTOR signaling was activated by LP and needed for the migration and proliferation of ARPE-19 cells. mTOR inhibition with rapamycin reduces the pro-proliferative effect of laser treatment on ARPE-19 cells, as well as the cell regeneration. These results suggest the mTOR pathway as a potential therapeutic target for various retinal disorders with proliferative component.

Methods

Cell culture The human adult RPE cell line (ARPE-19) was purchased from the American Type Culture Collection (Manassas, Virginia). The cells were seeded at a density of 5×10^5 cell/ml in 35-mm confocal dishes in Dulbecco's Modified Eagle Medium: F12 with 2.5 mM L-glutamine, 15 mM HEPES buffer (HyClone Lab., Logan, Utah) and supplemented with 10% fetal bovine serum (Gibco, Life Technologies, Grand Island, NY), 1% penicillin/streptomycin (GenDEPOT, Barker, TX), and incubated in a humidified 5% CO_2 atmosphere at 37 °C. The complete medium was changed every 2–3 days. The treatment was carried out with cultures reached 100% confluency.

Reagents and antibodies Rapamycin (Sigma-Aldrich Corp., St. Louis, MO) dissolved in dimethyl sulfoxide (DMSO, Sigma-Aldrich Corp., St. Louis, MO) was used at indicated concentrations.

The following antibodies were used: mTOR, p-mTOR S2481, p-S6, AKT, and p-AKT from Cell Signaling Technology (Danvers, MA); p-mTOR S2448 and vimentin from Abcam (Cambridge, UK); N-cadherin (Invitrogen Corp, Carlsbad, CA); IQGAP1 and GAPDH from Santa Cruz Biotechnology (Santa Cruz, CA).

Laser photocoagulation and rapamycin/DMSO vehicle treatment LP was performed as previously described with some modifications [5]. Shortly, the medium was removed from the wells and pre-sterilized black paper was put on the cells. The slit lamp delivery system of PASCAL diode laser (Topcon Medical Laser Systems, Livermore, CA) was used for LP with following settings: power intensity 350 mW, spot size 200 μm, and irradiation time 0.15 s. Each 35-mm dish was exposed to 50 evenly distributed laser shots. The complete medium with rapamycin at concentrations of 40, 80, 160 ng/ml, or DMSO vehicle was added after removal of black paper and kept in incubator up to specified time points.

Monitoring of the laser zone recovery and cell size/density analysis Images of laser spots were acquired using Zeiss Axio Observer A1 inverted microscope (Carl Zeiss, Oberkochen, Germany) equipped with AxioCam MRm monochrome digital camera (Carl Zeiss, Oberkochen, Germany) at 0, 12, 24, 72, and 120 h after LP and rapamycin or DMSO vehicle treatment. Laser-treated zone size was manually measured using ImageJ software (National Institutes of Health, Bethesda, MD). Briefly, the laser-treated zone was

selected with "Freehand selection" tool and measured considering the scale of the image; the data are presented as mean area ± SEM. The cells from four fields of each image were manually calculated (ImageJ software, NIH, Bethesda, MD) for cell length and density. The cell density was estimated as the mean number of cells per field. All figures were normalized to baseline values in percentage.

Cell viability assay Cell viability evaluated by 3-(4,5-dimethylthiazol-2-yl)-2,5-diphenyltetrazolium bromide (MTT assay) using EZ-Cytox Enhanced Cell Viability Assay Kit (DoGenBio Co., Ltd., Seoul, Korea). The cells were seeded at a density of 1×10^6 cell/ml in 96-well plates, and 24 h later after attaching, the cultured cells were subjected to LP (4 laser shots/well) and treated with rapamycin at different concentrations (40, 80, 160 ng/ml) or DMSO vehicle; untreated cell cultures were used as baseline. After 24, 72, and 120 h, the cells were incubated for 4 h after addition of 10 μl of MTT solution (5 μg/ml), and optical density was evaluated at 450 nm by VersaMax tunable microplate reader (Molecular Devices, Sunnyvale, CA). Cell viability was estimated as the ratio of the optical density of the treated cells to the untreated control in percentage.

EdU assay ARPE-19 cell proliferation after LP and treatment with rapamycin at concentrations of 40, 80, 160 ng/ml, or DMSO vehicle was assessed by EdU assay using Click-iT EdU® Alexa Fluor® 647 Imaging Kit (Invitrogen Corp, Carlsbad, CA) as described previously [28]. EdU-stained cells were visualized under the fluorescence microscope at × 100 magnifications and manually calculated using ImageJ software.

Immunoblotting analysis Western blot (WB) was performed using whole cell lysates from ARPE-19 cells exposed to laser and treated with rapamycin 160 ng/ml or DMSO vehicle; untreated cell cultures were used as a baseline. Cells were washed with cold Dulbecco's Phosphate-Buffered Saline (WELGENE, Gyeongsan, South Korea) before lysis in RIPA II lysis buffer with Triton, without EDTA (GenDEPOT, Barker, TX) supplemented with Xpert phosphatase inhibitor cocktail (GenDEPOT, Barker, TX) and Xpert protease inhibitor cocktail (GenDEPOT, Barker, TX). After 30 min incubation in lysis mixture, cell dish contents were transferred to a tube and centrifuged (13,000 rcf, 5 min, 4 °C); subsequently, the supernatant was allocated to a new tube and stored at − 80 °C.

Protein concentration was evaluated using BCA kit (Thermo Scientific, Middlesex, MA). Proteins were separated on SDS-polyacrylamide gel electrophoresis and transferred to PVDF membrane. Blocking and dilution solutions for primary and secondary antibodies were prepared as recommended by the manufacturers for each type of antibody. The blot was developed by Western blotting detection kit (Advansta, San Jose, CA) and acquired images of chemiluminescence were analyzed for densitometry values with ImageJ software. All data were normalized against GAPDH.

Immunofluorescence assay Twenty-four and 120 h after LP and treatment with rapamycin 160 ng/ml or DMSO vehicle, the cell cultures were fixed with 4% paraformaldehyde (PFA) in 0.1 M phosphate buffer (Biosesang, Seongnam, South Korea) for 15 min at room temperature. Samples were incubated in 0.1% Triton X-100 in PBS (PBST, Sigma-Aldrich Corp., St. Louis, MO) for 15 min, blocked in 1% skim milk in PBST for 1 h. Next, cells were exposed to primary antibodies (1:1000) for 2 h and then to secondary antibody—Alexa Fluor® 488 anti-rabbit dye (1:1000; Invitrogen Corp, Carlsbad, CA)—for 2 h at room temperature in the dark; nuclear counterstaining was performed with Hoechst 33342 (1:2000) in PBS.

Statistical analysis The repeated measures ANOVA with post hoc analysis was performed to compare the laser area recovery rate among experimental groups. The Wilcoxon signed-rank test was used to compare the cell size between groups. Statistical significance for cell density analysis, WB analysis, and viability assay was calculated using the Mann-Whitney *U* test. The Kruskal-Wallis test with post hoc analysis was performed for a comparison of EdU-positive cell number among experimental groups. Statistical analysis was performed with the IBM SPSS Statistics software (ver. 22, IBM Corp., Armonk, NY). Differences were considered statistically significant when $P \leq 0.05$.

Results

Rapamycin retards the recovery of laser photocoagulated area by ARPE-19 cells

The photothermal effect of laser resulted in the formation of empty spots and cell debris rim at the site of exposure (mean area 130,689.7 ± 5074.6 μm^2, $n = 120$). Repopulation of the RPE cells led to a reduction of empty spot size at early 12 and 24 h of observation at relatively equal pace in all groups; however, at 72 h of monitoring, laser spot recovery significantly decreased in rapamycin-treated groups in a concentration-dependent manner (Fig. 1a $P \leq 0.01$). While the laser spots in the control group are completely covered with the RPE cells at 120 h, lesion areas of rapamycin-treated groups still had empty regions in a dose-dependent manner ($P \leq 0.01$). As shown in Fig. 1a, b, 160 ng/ml concentration of rapamycin had the most prominent suppressive effect on lesion healing of

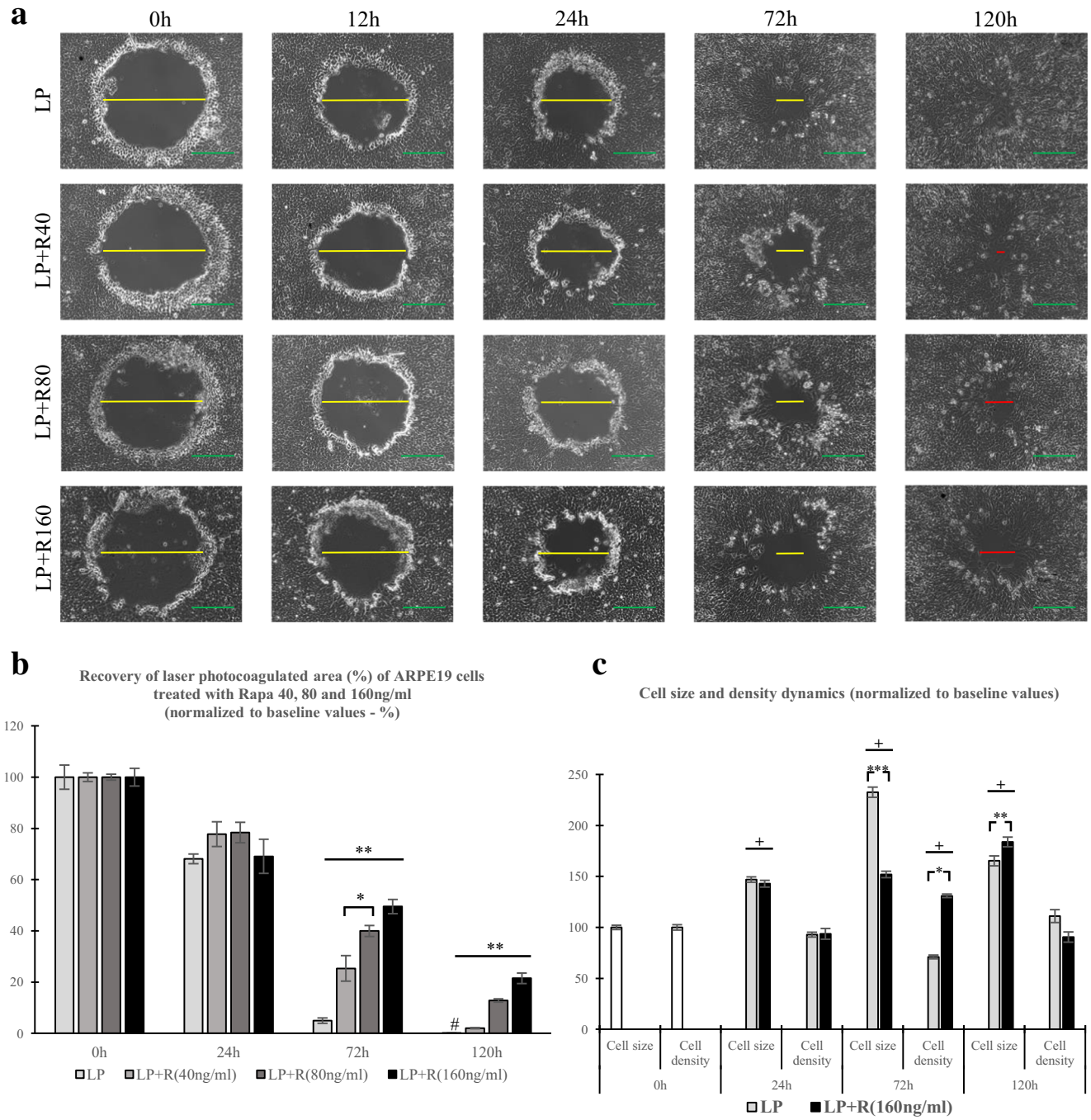

Fig. 1 Rapamycin retards the recovery of laser photocoagulated area by ARPE-19 cells. **a** Rapamycin markedly slows the restoration of the laser ablation zone by retinal epithelial cells in a concentration-dependent manner. *Scale bars*: *yellow*, the diameter of the laser spot of the control group at specified time points; *red*, the diameter of the laser zone of rapamycin-treated groups with definite concentrations; *green*, 200 μm. **b** In all groups, mean LP area at 0, 12, and 24 h of observation demonstrated relative equal numbers; however, 72 and 120 h data of rapamycin-treated groups significantly differ from completely recovered controls. Number sign indicates laser photocoagulated area in the control group totally recovered at 120 h of observation; Asterisk indicates $P \leq 0.05$; double asterisks indicate $P \leq 0.01$. Bars represent as the mean ± SEM from three independent experiments. **c** ARPE-19 cell size and density analysis revealed a significant difference in the center from images of control and LP + rapamycin (160 ng/ml) groups. Asterisk indicates $P \leq 0.05$; double asterisks indicate $P \leq 0.01$; triple asterisks indicate $P \leq 0.001$; plus sign indicates compared to 0 h values $P \leq 0.001$

ARPE-19 cells, almost 21% of the photocoagulated area remained empty ($P \leq 0.01$). Despite the fact that rapamycin at 40 and 80 ng/ml depicted significantly retarding effect on the recovery rate of ARPE-19 cells compared with the control group, they were less effective than rapamycin at higher concentration ($P \leq 0.01$).

Since LP + rapamycin 160 ng/ml group showed the lowest rate of recovery of the laser ablation zone, we compared the density and cell size around the laser spot with DMSO-treated cell values. The cells surrounding the laser spot in the control group rapidly increased in length and reached their peak (2.4 times longer than initial values) at 72 h. Corresponding to the complete repair of the empty area, the cell size decreased 120 h after LP, retaining significantly longer size comparing to initial values ($P \leq 0.001$). On the other hand, rapamycin-exposed cell length increased at a slower pace than DMSO-treated cells and reached 2/3 of control group cell length at 120 h ($P \leq 0.001$). In contrast, cell density values were less dynamic than cell size values. At 72 h, LP control group had significantly lower cell density comparing to baseline ($P \leq 0.001$), while the rapamycin-treated group demonstrated significantly higher density at the same time point ($P \leq 0.001$).

The dynamics of IQGAP1, N-cadherin, and vimentin expression in the RPE cell response to LP

To evaluate the dynamics of migration-related proteins after LP, we assessed the expression of IQGAP1, vimentin, and N-cadherin in the RPE cell cultures after LP and DMSO vehicle treatment (Fig. 2a, b). The induction of IQGAP1 expression after laser treatment at 12 h followed by downregulation up to 120 h (Fig. 2a, b-1). Vimentin expression demonstrated a similar trend as IQGAP1; however, at 120 h, its level was higher than at 72 h (Fig. 2a, b-2). N-cadherin level was downregulated from 12 to 120 h (Fig. 2a, b-2).

Since IQGAP1 and vimentin levels were the highest at 12 h, next, we compared IQGAP1, vimentin, and N-cadherin levels between LP control and LP + rapamycin 160 ng/ml treated groups at 12 h. As shown in Fig. 2c, d, mTOR inhibition with rapamycin treatment prevented upregulation of IQGAP1 and vimentin, while N-cadherin level was higher than LP control group at 12 h.

Rapamycin decreases the viability and proliferation of ARPE-19 cells after LP

ARPE-19 cell viability values were considerably lower in all laser-treated groups 24 h after LP compared with baseline ($P \leq 0.001$) (Fig. 3a), indicating a detrimental effect of LP on cell survival capacities. At 72 h, retinal pigment epithelial cell viability was significantly lower in rapamycin-treated groups compared to laser control; however, no significant difference was found in comparison among the groups treated with rapamycin. A similar trend was observed at 120 h of monitoring except for the viability values of cells treated with rapamycin at 40 ng/ml concentration, which demonstrated less toxicity than higher concentrations in comparison with laser control ($P \leq 0.05$) (Fig. 3a).

EdU assay results revealed significantly lower proliferation in all groups compared to baseline values at 24 h ($P \leq 0.001$) (Fig. 3b, c). LP control and LP + rapamycin 40 ng/ml groups had significantly higher proliferation compared to untreated cells at 72 and 120 h, whereas EdU-positive cell numbers in LP + rapamycin 80 and 160 ng/ml groups were similar to baseline (Fig. 3b).

The effect of rapamycin on the mTOR pathway in ARPE-19 cell after LP

To elucidate the role of the mTOR pathway in the RPE cell response to LP, mTOR, S6, and AKT phosphorylation levels were analyzed by WB (Fig. 4a, b). Total mTOR level was slightly upregulated in laser + DMSO vehicle-treated group, but the difference was significant at 120 h (Fig. 4a, b-1) ($P \leq 0.05$). Meanwhile, total mTOR level gradually decreased in LP + rapamycin-treated group over the observation period ($P \leq 0.05$). LP upregulated mTOR phosphorylation on Ser 2448 (p-mTOR S2448) in the control group at 12 h and remained at about the same level for the rest of the observation period (Fig. 4a, b-2). Rapamycin treatment significantly suppressed the laser-induced activation of mTOR, since p-mTOR S2448 level was below the baseline values at 12 h, continuing to decrease up to 120 h ($P \leq 0.05$). However, at 72 and 120 h, decline was less than total mTOR reduction ($P \leq 0.05$) (Fig. 4b-2).

S6 phosphorylation on Ser240/244 level considerably increased at 12 and 24 h following LP and dropped at 72 h maintaining significantly higher level compared to baseline up to the end of the observation period ($P \leq 0.05$) (Fig. 4b-3). As expected from mTOR inhibition, rapamycin-treated cells showed a significantly lower level of p-S6 at 24, 72, and 120 h compared to LP control group ($P \leq 0.05$) (Fig. 4b-1, 2). Next, we measured the expression levels of phosphorylated mTOR on S2481 (p-mTOR S2481). LP significantly induced p-mTOR S2481 level in both groups and kept high in LP control group for the rest of the study period ($P \leq 0.05$). Rapamycin treatment significantly reduced p-mTOR S2481 level at 24 h and this reduction was maintained up to 120 h ($P \leq 0.05$) (Fig. 4b-3). Total AKT was upregulated following laser treatment in both groups with significant predominance in the rapamycin-treated group ($P \leq 0.05$) (Fig. 4b-5). Laser treatment significantly inhibited the phosphorylation of AKT on S473 (p-AKT S473) in both groups ($P \leq 0.05$). However, LP + rapamycin group demonstrated higher levels of p-AKT S473 compared to LP control group, but only 12-h results were statistically significant ($P \leq 0.05$) (Fig. 4b-6). These data confirm the activation of the mTOR signaling pathway in ARPE-19 cells upon laser damage.

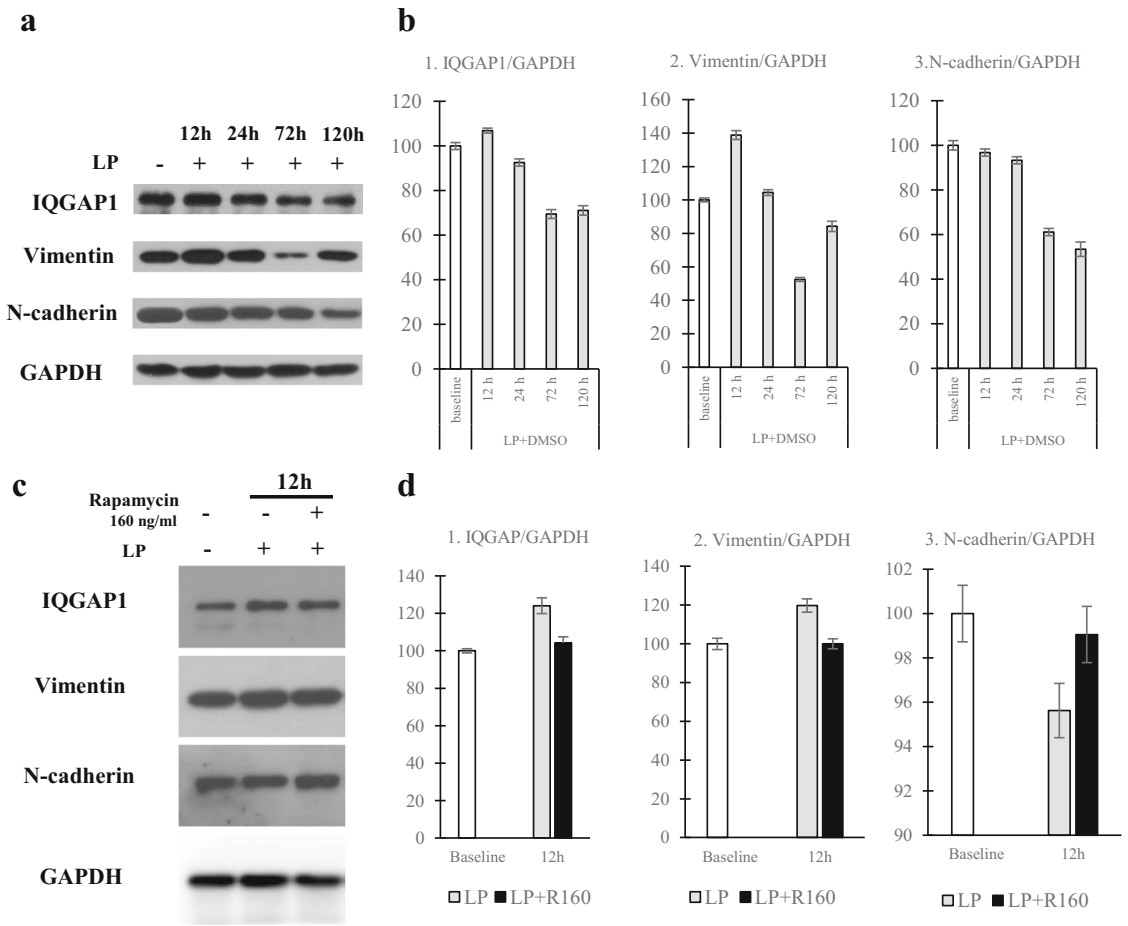

Fig. 2 The expression of EMT-related proteins in the RPE cells after laser photocoagulation. **a**, **c** Western blot analysis of IQGAP1, vimentin, N-cadherin, and GAPDH. **b**, **d** Quantitative analysis of the results of Western blot using ImageJ. Protein levels were normalized to GAPDH. Bars represent as the mean ± SEM from three independent experiments

Immunofluorescence staining of ARPE-19 cells for p-mTOR S2448 and p-S6

Immunofluorescence staining of ARPE-19 cells for p-mTOR S2448 and p-S6 antibodies also confirmed mTOR pathway upregulation in laser-exposed cell cultures and rapamycin treatment inhibited the phosphorylation of mTOR and ribosomal S6 proteins (Fig. 5a, b).

Discussion

The mechanistic target of rapamycin—a major coordinator of cell growth and proliferation—has been shown to play a critical role in epithelial-mesenchymal transition and migration of various cancer cells [29, 30]. Recently, it has been reported that mTOR inhibition impaired the RPE cell migration in a dose-dependent manner [31]. In the current study, we revealed a significant reduction in the recovery of laser area in rapamycin-treated groups at 72 and 120 h in a dose-dependent manner ($P \leq 0.05$) (Fig. 1a, b). Analyzing the cell size dynamics, we found that neighboring cells to the lesion area rapidly elongated with the longest value at 72 h and retained significantly longer size even the laser spots were completely repopulated with ARPE-19 cells in the control group at 120 h (Fig. 1a and c). On the other hand, LP + rapamycin 160 ng/ml treated cells increased in length at a substantially slower pace compared to LP + DMSO control (Fig. 1c), indirectly indicating the altered migratory ability due to mTOR inhibition.

The RPE cells acquire the ability to migrate via epithelial-mesenchymal transition (EMT). This process includes loss of adherent junctions between cells, cytoskeleton reorganization with alteration of cell polarity to form spindle-shaped mesenchymal cells [32, 33]. IQGAP1—a multifunctional protein, which has a crucial role in the regulation of cytoskeleton organization—has also been found to be an element of the mTOR pathway that regulates cell size and growth [34]. Our results demonstrated that laser-induced upregulation of IQGAP1 is reversed with rapamycin treatment (Fig. 2c, d-1).

The loss of adhesion junctions is characterized by the loss of expression of cadherin homodimers [35, 36]. It has been

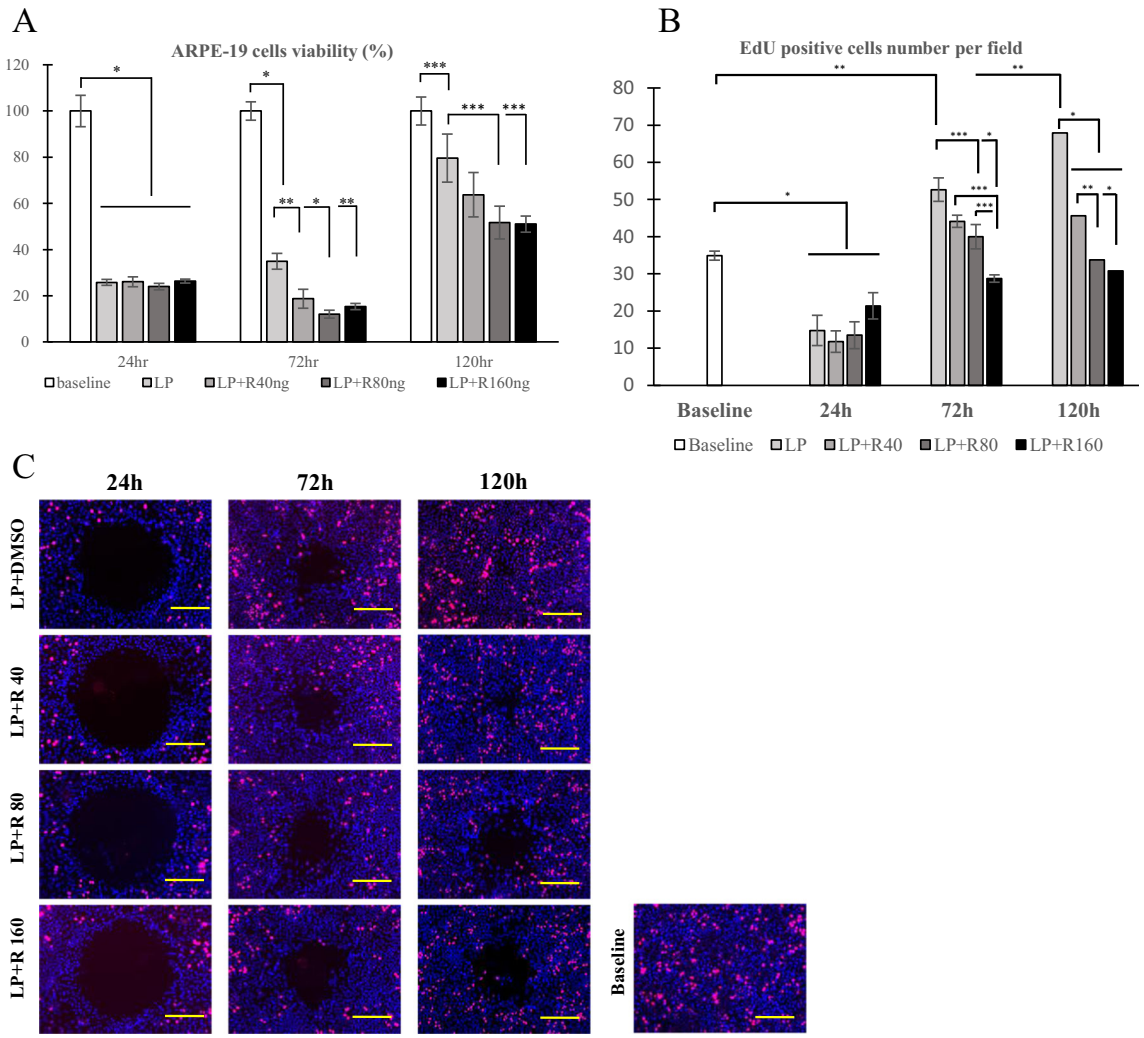

Fig. 3 Rapamycin decreases the viability and proliferative activity of ARPE-19 cells after LP. **a** MTT assay results showed that ARPE-19 cell viability decreased in all laser-exposed groups compared to the baseline group (without laser, without rapamycin). Early observations at 24 h depicted no significant difference between laser-treated groups. Further observation at 72 and 120 h of monitoring revealed significantly lower viability values in rapamycin-treated groups comparing to laser control. Asterisk indicates $P \leq 0.001$; double asterisks indicate $P \leq 0.01$; triple asterisks indicate $P \leq 0.05$; Bars represent as the mean ± SEM from three independent experiments. **b**, **c** EdU assay was used to evaluate the effect of rapamycin on the proliferation of ARPE-19 cells after laser ablation. All groups were treated with EdU 5 μM/l solution as well as rapamycin with indicated concentrations or DMSO vehicle immediately after LP. Asterisk indicates $P \leq 0.001$; double asterisks indicate $P \leq 0.01$; triple asterisks indicate $P \leq 0.05$; Bars represent as the mean number of EdU-stained cells per field ± SEM from three independent experiments. Scale bars 200 μm

found that N-cadherin, among other subtypes, is predominantly expressed in cultured human RPE cells [37, 38]. Therefore, we detected N-cadherin after laser treatment and suppressed expression indicated a loss of epithelial characteristics of the RPE cell and a transdifferentiation toward mesenchymal phenotype (Fig. 2c, d-3). Another hallmark of EMT is an increased expression of vimentin—an intermediate filament protein, mainly expressed in mesenchymal cells. In our experiments, laser exposure induced the expression of vimentin, and mTOR inhibition could prevent this effect at 12 h (Fig. 2c, d-2). Based on these findings, it can be assumed that LP initiates EMT of ARPE-19 cells, and mTOR pathway is involved in the regulation of laser-induced cell migration.

It has also been reported that the mTOR signaling pathway is involved in the RPE cell response under stress conditions [23, 39]. Moreover, it was demonstrated that the upregulation of mTOR signaling against oxidative stress corresponds to the complete recovery of the RPE cells [23]. Our results of WB analysis revealed the induction of phosphorylation of mTOR upon laser treatment; accordingly, cell viability was significantly higher than mTOR-inhibited groups at 72 and 120 h (Fig. 4a, b-2 and Fig. 3a). It should be noted that a dose-dependent decrease in cell viability after laser treatment was found at concentrations depicted as safe for the RPE cell (Liegl R. et al. utilized temsirolimus, an ester derivative of

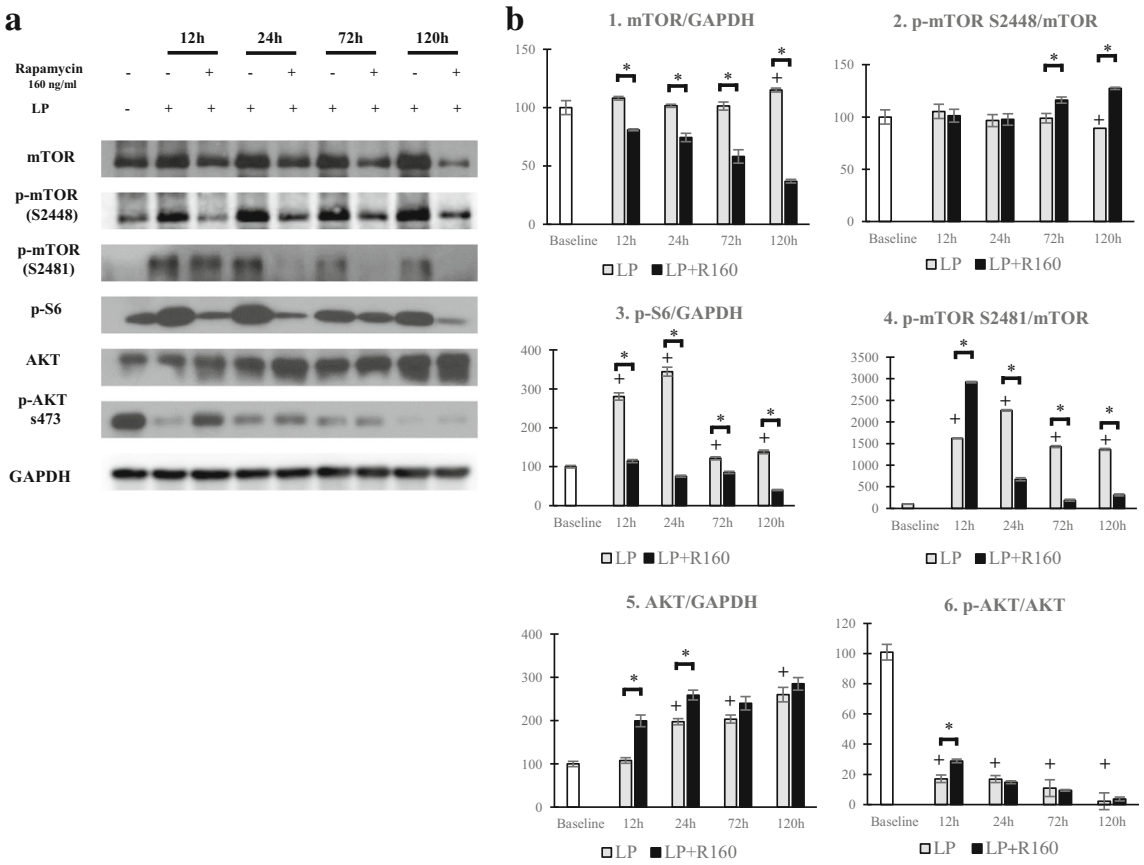

Fig. 4 The effect of rapamycin at the concentration of 160 ng/ml on mTOR pathway in ARPE-19 cell after LP. **a** Western blot analysis of total mTOR, p-mTOR (S2448), p-mTOR (S2481), p-S6, AKT, p-AKT, and GAPDH. **b** Quantitative analysis of the results of Western blot using ImageJ. Protein levels were normalized to GAPDH. Plus sign indicates comparison between baseline and LP control, $P \leq 0.05$; asterisk indicates comparison between LP group and LP + Rapa 160 ng/ml, $P \leq 0.05$; bars represent as the mean ± SEM from three independent experiments

rapamycin was found to be non-toxic at much higher concentrations—0.005 to 12.5 μg/ml—than we used in our experiments) [31]. These findings indicate that mTOR pathway activation is essential for the RPE cell recovery after laser treatment.

Induction of the RPE cell proliferation upon laser treatment was previously shown by Tababat-Khani et al. [5]. In our experiments, we also confirmed the RPE cell proliferative activity arising from laser exposure and mTOR inhibition suppressed this activity in rapamycin-treated groups in a dose-dependent manner (Fig. 3b, c). At 24 h, the RPE cell proliferation was significantly decreased in all laser-treated groups; however, the process of lesion healing continued apparently due to the migration of adjacent cells to the damaged area. At 72 and 120 h, the proliferative activity of ARPE-19 cells in the LP control group was significantly higher than rapamycin-treated groups (Fig. 3b, c). Given the fact that at these time points rapamycin-treated groups demonstrated the substantial difference in the recovery rate of laser area (Fig. 1a, b), it can be assumed that proliferation has a significant contribution to the recovery processes at later time points after LP. Our data clearly demonstrated that mTOR is an important conductor of ARPE-19 cell behavior after laser treatment. Considering the facts that LP mimics the damage to the RPE cells and the role of mTOR pathway in the RPE cell recovery processes, it can be assumed that mTOR targeting may be used therapeutically against the retinal disorders with the proliferative component.

Further, we confirmed mTOR pathway activation after LP by WB analysis. p-mTOR S2448 level, mostly contained in mTORC1 [40], was upregulated after laser treatment and rapamycin treatment prevented its overexpression. It is increasingly obvious that prolonged rapamycin treatment can alter mTORC2 level, since 1-h exposure to rapamycin had no effect on mTORC2 level in contrast to 24-h treatment, which resulted in inhibition of mTORC2 assembly [41] and suppression of p-mTOR S2481 level, predominantly contained in mTORC2 [40]. In accordance with these data, we revealed that upregulated level of p-mTOR S2481 after laser exposure was significantly decreased with rapamycin treatment at 24 h and remained suppressed up to 120 h. Our results of WB

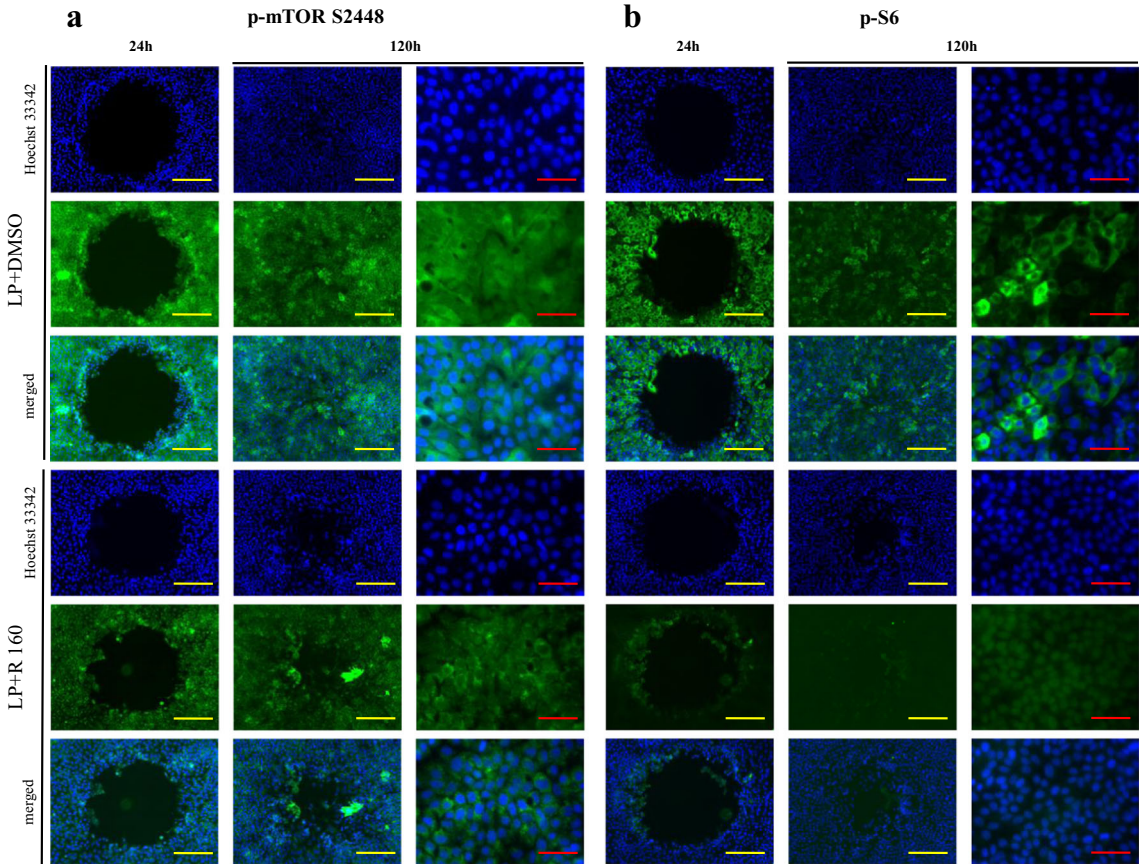

Fig. 5 Expression of p-mTOR S2448 and p-S6 in LP control and LP + rapamycin 160 ng/ml treated ARPE-19 cells. **a**, **b** Representative immunofluorescence images of p-mTOR S2448 and p-S6 protein in ARPE-19 cells exposed to laser photocoagulation with rapamycin 160 ng/ml or DMSO vehicle treatment at 24 and 120 h. Nuclear staining was performed with Hoechst 33342 (blue); p-mTOR S2448 and p-S6 proteins were labeled with Alexa Fluor® 488 dye (green). Imaging (× 100 and × 400 magnification) was made with Zeiss Axio Observer A1 inverted microscope equipped with AxioCam MRm monochrome digital camera and acquired images assembled with Zen 2.3 (blue edition) imaging software. *Scale bars*: *yellow* 200 μm, *red* 50 μm

suggest that both mTORC1 and mTORC2 are involved in lesion healing process after LP. We also analyzed the phosphorylation level of S6, a downstream target of both mTOR and ERK signaling pathways (Fig. 4a, b-3) [42]. In laser control group, p-S6 level was substantially increased at 12 h and reached its peak at 24 h, while p-mTOR level significantly upregulated at 12 h and remained at about the same level up to 120 h. A certain portion of phosphorylation of S6 in our experiments might be induced by ERK pathway activation due to compensatory cross-talk between mTOR and ERK pathways [43].

Recently, the results of two sequential phase-3 clinical trial—Sirolimus study Assessing double-masKed Uveitis tReAtment (SAKURA) study—were published, which supports the efficacy and safety of rapamycin (sirolimus) in noninfectious uveitis [44]. Our experiments also demonstrate that mTOR pathway could be targeted for wide therapeutic applications, such as prevention/treatment of retinal disorders with the proliferative component. Our findings are particularly interesting since the combination of laser treatment with mTOR inhibition may have a potential therapeutic effect in advanced cases of diabetic retinopathy, retinal vein occlusion, and retinopathy of prematurity.

In conclusion, our study shows the first evidence of laser-induced mTOR pathway activation in ARPE-19 cell, which is essential for the regulation of cell migration and proliferation. In addition, mTOR inhibition by rapamycin reduces the pro-proliferative effect of laser treatment on ARPE-19 cells and diminishes the restorative capabilities of ARPE-19 cells, as well as affecting the viability.

Funding information This research was supported by a grant from the Korea Health Technology R&D Project through the Korea Health Industry Development Institute (KHIDI), funded by the Ministry of Health and Welfare (grant number HI17C0966); a grant from Basic Science Research Program through the National Research Foundation of Korea (NRF) funded by the ministry of Education, Science, and Technology (No.2016R1A2B4008376; Seoul, Republic of Korea); and also partially supported by the Soonchunhyang University research fund.

Compliance with ethical standards

Conflict of interest The authors declare that they have no conflict of interest.

References

1. Diabetic Retinopathy Study Research Group (1978) Photocoagulation treatment of proliferative diabetic retinopathy: The second report of diabetic retinopathy study findings. Ophthalmology 85:82–106. https://doi.org/10.1016/S0161-6420(78)35693-1
2. Early Treatment Diabetic Retinopathy Study research group (1987) Treatment techniques and clinical guidelines for photocoagulation of diabetic macular edema. Early Treatment Diabetic Retinopathy Study report number 2. Ophthalmology 94:761–774
3. Good WV, Early Treatment for Retinopathy of Prematurity Cooperative Group (2004) Final results of the Early Treatment for Retinopathy of Prematurity (ETROP) randomized trial. Trans Am Ophthalmol Soc 102:233–248 discussion 248–50
4. Priebe LA, Cain CP, Welch AJ (1975) Temperature rise required for production of minimal lesions in the Macaca mulatta retina. Am J Ophthalmol 79:405–413. https://doi.org/10.1016/0002-9394(75)90613-3
5. Tababat-Khani P, Berglund LM, Agardh CD, Gomez MF, Agardh E (2013) Photocoagulation of human retinal pigment epithelial cells in vitro: evaluation of necrosis, apoptosis, cell migration, cell proliferation and expression of tissue repairing and cytoprotective genes. PLoS One 8(8):e70465. https://doi.org/10.1371/journal.pone.0070465
6. Campochiaro PA (2000) Retinal and choroidal neovascularization. J Cell Physiol 184:301–310. https://doi.org/10.1002/1097-4652(200009)184:3<301::AID-JCP3>3.0.CO;2-H
7. Duh EJ, Yang HS, Haller JA, De Juan E, Humayun MS, Gehlbach P, Melia M et al (2004) Vitreous levels of pigment epithelium-derived factor and vascular endothelial growth factor: implications for ocular angiogenesis. Am J Ophthalmol 137(4):668–674. https://doi.org/10.1016/j.ajo.2003.11.015
8. Strauss O (2005) The retinal pigment epithelium in visual function. Physiol Rev 85(3):845–881. https://doi.org/10.1152/physrev.00021.2004
9. Sparrow JR, Hicks D, Hamel CP (2010) The retinal pigment epithelium in health and disease. Curr Mol Med 10(9):802–823. https://doi.org/10.2174/156652410793937813
10. Muether PS, Neuhann I, Buhl C, Hermann MM, Kirchhof B, Fauser S (2013) Intraocular growth factors and cytokines in patients with dry and neovascular age-related macular degeneration. Retina 33(9):1809–1814. https://doi.org/10.1097/IAE.0b013e318285cd9e
11. Kernt M, Neubauer AS, Liegl RG, Hirneiss C, Alge CS, Wolf A, Ulbig MW, Kampik A (2010) Sorafenib prevents human retinal pigment epithelium cells from light-induced overexpression of VEGF, PDGF and PlGF. Br J Ophthalmol 94(11):1533–1539. https://doi.org/10.1136/bjo.2010.182162
12. Hattenbach LO, Beck KF, Pfeilschifter J, Koch F, Ohrloff C, Schacke W (2005) Pigment-epithelium-derived factor is upregulated in photocoagulated human retinal pigment epithelial cells. Ophthalmic Res 37(6):341–346. https://doi.org/10.1159/000088263
13. Polivka J Jr, Janku F (2014) Molecular targets for cancer therapy in the PI3K/AKT/mTOR pathway. Pharmacol Ther 142(2):164–175. https://doi.org/10.1016/j.pharmthera.2013.12.004
14. Kim YC, Guan KL (2015) mTOR: a pharmacologic target for autophagy regulation. J Clin Invest 125(1):25–32. https://doi.org/10.1172/JCI73939
15. Perl A (2015) mTOR activation is a biomarker and a central pathway to autoimmune disorders, cancer, obesity, and aging. Ann N Y Acad Sci 1346(1):33–44. https://doi.org/10.1111/nyas.12756
16. Johnson SC, Rabinovitch PS, Kaeberlein M (2013) mTOR is a key modulator of ageing and age-related disease. Nature 493(7432):338–345. https://doi.org/10.1038/nature11861
17. Laplante M, Sabatini DM (2012) mTOR signaling in growth control and disease. Cell 149(2):274–293. https://doi.org/10.1016/j.cell.2012.03.017
18. Jing L, Sang GK, Blenis J (2014) Rapamycin: one drug, many effects. Cell Metab 19(3):373–379. https://doi.org/10.1016/j.cmet.2014.01.001
19. Zhao C, Vollrath D (2011) mTOR pathway activation in age-related retinal disease. Aging (Albany NY) 3(4):346–347. https://doi.org/10.18632/aging.100303
20. Jacot JL, Sherris D (2011) Potential therapeutic roles for inhibition of the PI3K/Akt/mTOR pathway in the pathophysiology of diabetic retinopathy. J Ophthalmol 2011:589813
21. Yagasaki R, Nakahara T, Ushikubo H, Mori A, Sakamoto K, Ishii K (2014) Anti-angiogenic effects of mammalian target of rapamycin inhibitors in a mouse model of oxygen-induced retinopathy. Biol Pharm Bull 37(11):1838–1842. https://doi.org/10.1248/bpb.b14-00487
22. Çakmak H, Ergin K, Bozkurt G, Kocatürk T, Evliçoğlu GE (2016) The effects of topical everolimus and sunitinib on corneal neovascularization. Cutan Ocul Toxicol 35(2):97–103
23. Faghiri Z, Bazan NG (2010) PI3K/Akt and mTOR/p70S6K pathways mediate neuroprotectin D1-induced retinal pigment epithelial cell survival during oxidative stress-induced apoptosis. Exp Eye Res 90(6):718–725 https://doi.org/10.1016/j.exer.2010.03.002
24. Dunn KC, Aotaki-Keen AE, Putkey FR, Hjelmeland LM (1996) ARPE-19, a human retinal pigment epithelial cell line with differentiated properties. Exp Eye Res 62:155–169. https://doi.org/10.1006/exer.1996.0020
25. Hamel CP, Tsilou E, Pfeffer BA, Hooks JJ, Detrick B, Redmond TM (1993) Molecular cloning and expression of RPE65, a novel retinal pigment epithelium-specific microsomal protein that is post-transcriptionally regulated in vitro. J Biol Chem 268:15751–15757
26. Finnemann SC, Bonilha VL, Marmorstein AD, RodriguezBoulan E (1997) Phagocytosis of rod outer segments by retinal pigment epithelial cells requires alpha(v)beta5 integrin for binding but not for internalization. Proc Natl Acad Sci U S A 94:12932–12937. https://doi.org/10.1073/pnas.94.24.12932
27. Park TK, Lee SH, Choi JS, Nah SK, Kim HJ, Park HY, Lee H, Lee SHS, Park K (2017) Adeno-associated viral vector-mediated mTOR inhibition by short hairpin RNA suppresses laser-induced choroidal neovascularization. Mol Ther Nucleic Acids 8:26–35. https://doi.org/10.1016/j.omtn.2017.05.012
28. Oh JR, Han JW, Kim YK, Ohn YH, Park TK (2017) The effects of anti-vascular endothelial growth factor agents on human retinal pigment epithelial cells under high glucose conditions. Int J Ophthalmol 10(2):203–210
29. Zong H, Yin B, Zhou H, Cai D, Ma B, Xiang Y (2014) Inhibition of mTOR pathway attenuates migration and invasion of gallbladder cancer via EMT inhibition. Mol Biol Rep 41(7):4507–4512. https://doi.org/10.1007/s11033-014-3321-4
30. Han B, Cui H, Kang L, Zhang X, Jin Z, Lu L, Fan Z (2015) Metformin inhibits thyroid cancer cell growth, migration, and EMT through the mTOR pathway. Tumour Biol 36(8):6295–6304. https://doi.org/10.1007/s13277-015-3315-4
31. Liegl R, Koenig S, Siedlecki J, Haritoglou C, Kampik A, Kernt M (2014) Temsirolimus inhibits proliferation and migration in retinal pigment epithelial and endothelial cells via mTOR inhibition and

decreases VEGF and PDGF expression. PLoS One 9(2):e88203. https://doi.org/10.1371/journal.pone.0088203
32. Briggs MW, Sacks DB (2003) IQGAP proteins are integral components of cytoskeletal regulation. EMBO Rep 4(6):571–574. https://doi.org/10.1038/sj.embor.embor867
33. Noritake J, Watanabe T, Sato K, Wang S, Kaibuchi K (2005) IQGAP1: a key regulator of adhesion and migration. J Cell Sci 118(Pt 10):2085–2092. https://doi.org/10.1242/jcs.02379
34. Wang JB, Sonn R, Tekletsadik YK, Samorodnitsky D, Osman MA (2009) IQGAP1 regulates cell proliferation through a novel CDC42-mTOR pathway. J Cell Sci 122(Pt 12):2024–2033. https://doi.org/10.1242/jcs.044644
35. McCrea PD, Maher MT, Gottardi CJ (2015) Nuclear signaling from cadherin adhesion complexes. Curr Top Dev Biol 112:129–196. https://doi.org/10.1016/bs.ctdb.2014.11.018
36. Kalluri R, Weinberg RA (2009) The basics of epithelial-mesenchymal transition. J Clin Invest 119(6):1420–1428. https://doi.org/10.1172/JCI39104
37. McKay BS, Irving PE, Skumatz CM, Burke JM (1997) Cell-cell adhesion molecules and the development of an epithelial phenotype in cultured human retinal pigment epithelial cells. Exp Eye Res 65(5):661–671. https://doi.org/10.1006/exer.1997.0374
38. Youn YH, Hong J, Burke JM (2006) Cell phenotype in normal epithelial cell lines with high endogenous N-cadherin: comparison of RPE to an MDCK subclone. Invest Ophthalmol Vis Sci 47(6):2675–2685. https://doi.org/10.1167/iovs.05-1335
39. Liu NN, Zhao N, Cai N (2015) Suppression of the proliferation of hypoxia-induced retinal pigment epithelial cell by rapamycin through the /mTOR/HIF-1α/VEGF/ signaling. IUBMB Life 67(6):446–452. https://doi.org/10.1002/iub.1382
40. Copp J, Manning G, Hunter T (2009) TORC-specific phosphorylation of mTOR: phospho-Ser2481 is a marker for intact mTOR-C2. Cancer Res 69(5):1821–1827. https://doi.org/10.1158/0008-5472.CAN-08-3014
41. Sarbassov DD, Ali SM, Sengupta S, Sheen JH, Hsu PP, Bagley AF, Markhard AL, Sabatini DM (2006) Prolonged rapamycin treatment inhibits mTORC2 assembly and Akt/PKB. Mol Cell 22(2):159–168. https://doi.org/10.1016/j.molcel.2006.03.029
42. Pende M, Um SH, Mieulet V, Sticker M, Goss VL, Mestan J, Mueller M, Fumagalli S, Kozma SC, Thomas G (2004) S6K1(-/-)/S6K2(-/-) mice exhibit perinatal lethality and rapamycin-sensitive 5′-terminal oligopyrimidine mRNA translation and reveal a mitogen-activated protein kinase-dependent S6 kinase pathway. Mol Cell Biol 24(8):3112–3124. https://doi.org/10.1128/MCB.24.8.3112-3124.2004
43. Butler DE, Marlein C, Walker HF et al (2017) Inhibition of the PI3K/AKT/mTOR pathway activates autophagy and compensatory Ras/Raf/MEK/ERK signalling in prostate cancer. Oncotarget 8(34):56698–56713. https://doi.org/10.18632/oncotarget.18082
44. Nguyen QD, Merrill PT, Clark WL, Banker AS, Fardeau C, Franco P, LeHoang P, Ohno S et al (2016) Intravitreal Sirolimus for non-infectious uveitis: a phase III Sirolimus study Assessing double-masKed Uveitis TReAtment (SAKURA). Ophthalmology 123(11):2413–2423. https://doi.org/10.1016/j.ophtha.2016.07.029